AIAA AVIATION Forum
5-9 June 2017, Denver, Colorado
17th AIAA Aviation Technology, Integration, and Operations Conference

10.2514/6.2017-3990

Time-Coordination Strategies and Control Laws for Multi-Agent Unmanned Systems

Javier Puig-Navarro*, Naira Hovakimyan†
University of Illinois at Urbana-Champaign, Urbana, IL, 61801, USA
B. Danette Allen‡
NASA Langley Research Center, Hampton, VA, 23681, USA

Time-critical coordination tools for unmanned systems can be employed to enforce the type of temporal constraints required in terminal control areas, ensure minimum distance requirements among vehicles are satisfied, and successfully perform coordinated missions. In comparison with previous literature, this paper presents an ampler spectrum of coordination and temporal specifications for unmanned systems, and proposes a general control law that can enforce this range of constraints. The constraint classification presented considers the nature of the desired arrival window and the permissible coordination errors to define six different types of time-coordination strategies. The resulting decentralized coordination control law allows the vehicles to negotiate their speeds along their paths in response to information exchanged over the communication network. This control law organizes the different members in the fleet per their behavior and informational needs as reference agent, leaders, and followers. Examples and simulation results for all the coordination strategies presented demonstrate the applicability and efficacy of the coordination control law presented here.

I. Introduction

Recent developments in unmanned systems (UxSs) technologies have opened vast opportunities in scientific research,[1–3] remote monitoring and control,[4] rapid assessment of catastrophic events,[5] search and rescue operations,[6,7] cartography,[8,9] and cinematography, to name a few examples. Not only have UxSs eliminated the constraints and limitations of manned vehicles, but also their relatively low cost, miniaturization levels, and ease of deployment have popularized their use in the aforementioned areas. Moreover, fleets of cooperating UxSs can be used to exploit synergistic behaviors among vehicles, remove the risk of single-point failures, improve flexibility, increase redundancy and reliability, achieve blanket coverage of larger areas, and often reduce mission execution times.

A fundamental component to achieve these goals is the availability of cooperative control strategies that are robust to temporary communication dropouts, packet loss, and external disturbances. Additionally, these cooperative strategies shall ensure safe inter-vehicle separation, while being able to adapt to changing mission goals, fleet size, and vehicle diversity. Technical advances in time coordination have the potential to realize new transportation paradigms that hold promise for revolutionary changes in other fields such as air traffic management,[10] mail services, and ground transportation systems.

Inspired by these challenges, previous work[11,12] developed a set of algorithms for time-critical cooperative path-following control of a fleet of unmanned aerial vehicles (UAVs) that exchange information over a communication network. The resulting framework divides the fleet into leaders and followers, and guarantees that the UAVs follow their assigned trajectories, while meeting temporal and spatial constraints. Moreover,

*Graduate Student, Dept. of Aerospace Engineering, 104 S. Wright St., Urbana, IL, AIAA Student Member.
†Professor, Dept. of Mechanical Science and Engineering, 1206 W. Green St., Urbana, IL, AIAA Fellow.
‡Senior Technologist for Intelligent Flight Systems, Crew Systems & Aviation Operations Branch, MS 492, AIAA Senior Member.

this set of algorithms allows UAVs to compensate for off-nominal situations by negotiating the speed along their paths.

In this paper, we focus on the time-coordination aspect of this framework. First developments[13] only considered tight coordination constraints among vehicles, leaving no room for bounded coordination errors among UxSs. Later work[14] combined tight coordination constraints with a variety of temporal constraints, such as a specific time of arrival or a desired window of arrival, for one or more points along the assigned paths. To achieve this, the reference agent was introduced[14] as a means to impose temporal specifications on the fleet of UxSs. This paper maintains the reference agent and expands the previous spectrum of time-coordination strategies.[14,15] In particular, loose coordination constraints are introduced and combined with prior coordination and temporal assignments, resulting in six general time-coordination strategies. The importance of loose coordination constraints relies in the fact that it explicitly allows bounded errors in the coordination among vehicles. The practicality of each strategy is illustrated through a real-world scenario. This paper proposes a new and broader control law that relies on the decision logic of a set of link weights to impose the desired set of coordination and temporal constraints. Moreover, the algorithm presented here provides all agents in the fleet with disturbance rejection capabilities. As a result, contrary to previous publications, leaders do not necessarily need to be virtual agents. This paper also presents simulation results that highlight the importance of imposing the appropriate set of temporal and coordination constraints. In fact, this paper provides numerical evidence that loose coordination is preferable over tight coordination since it leads to smaller speed corrections, and thus a reduction in fuel consumption. Numerical results also support a similar prioritization for the types of temporal constraints.

This paper is organized as follows. Section II presents a brief overview of the background and algorithms required to perform multi-vehicle cooperative missions, and their relation with the time-coordination strategies and protocols presented in this paper. Section III characterizes the time-coordination problem as a combination of a consensus and a collective tracking problem, and provides a physical interpretation of the resulting problem formulation. Section IV defines the set of coordination constraints and temporal specifications that lead to the definition of the time-coordination strategies presented in this paper. Examples of realistic missions that could be executed with these strategies are provided to motivate the applicability of this work. Section V proposes a novel distributed control law that enforces desired coordination constraints and temporal specifications on the fleet of UxSs. Section VI includes numerical simulation results that show the capabilities of the aforementioned control law. Finally, Section VII concludes the paper with a summary of the findings of this research, and recommendations regarding the application of the time-coordination algorithms.

II. Background: Time-Critical Cooperative Path Following

The goal of the aforementioned cooperative framework is to safely guide a fleet of UxSs along their assigned trajectories, while meeting predefined spatial and temporal constraints. Spatial constraints ensure vehicles do not collide with other fleet members or fixed obstacles, while temporal constraints enforce a desired schedule on the UxSs. Research in this area regarding ground,[16] underwater,[17–19] and aerial[12,20–22] vehicles has grown significantly in the last decade. The time-critical cooperative path-following framework is based on the idea of decoupling space and time, and is composed of three basic elements:

- **Trajectory generation algorithm**[23,24] is responsible for the computation of a geometrical path and a desired speed profile $v_{d,i}(t)$ for each of the n vehicles in the fleet, $i \in \mathcal{I} := \{1, \ldots, n\}$. Under nominal conditions, this algorithm ensures that UxSs maintain safe inter-vehicle separation, while complying with a set of vehicle-specific dynamic constraints, such as minimum and maximum speed or acceleration. To ensure that minimum spatial clearance among vehicles is maintained at all times, this algorithm provides two alternative solutions: *i*) spatial deconfliction, which ensures that the minimum distance between any two points on the paths is greater or equal than a minimum safety threshold; and *ii*) temporal deconfliction, which guarantees that the distance between any two vehicles is greater or equal than the minimum spatial clearance at all times, even though their corresponding paths may not be spatially deconflicted. To ensure that the vehicles maintain the desired relative position, and thus maneuvers are collision free, this type of deconfliction requires the vehicles to coordinate along their paths. The trajectory generation algorithm is vehicle specific, since it relies on optimization methods that take into account an optimization criterion, and a set of simplified dynamic constrains.

- **Path following algorithm**[12,22] ensures that UxSs converge to and follow their assigned paths, regardless of what the speed profile is, as long as it is physically feasible. Note that this algorithm is also vehicle-specific since path-following strategies vary for fixed-wing aircraft, multirotors, or watercraft, to mention but a few examples.

- **Time-coordination algorithm**[12,14] guarantees that vehicles in the fleet reach agreement on some distributed variables of interest. These parameters are referred to as the *coordination states* and denoted as $x_i(t) \in \mathbb{R}$, $i \in \mathcal{I}$. The coordination states and assigned trajectories capture the objectives of the cooperative mission, such as desired relative position among vehicles and temporal constraints. As in previous formulations,[12–14] the coordination states are scalar time-variables defined over the interval $[0, t^f_{d,i}]$, where $t^f_{d,i}$ is the desired nominal duration of the mission for the ith vehicle. These time-variables are defined to ensure that:

  - if any two vehicles i and j agree on their coordination states, namely $x_i(t) = x_j(t)$, then these two vehicles have the desired relative position along their paths at time t and, thus, satisfy the coordination constraints as specified by the trajectory-generation algorithm;
  - if $\dot{x}_i(t) = 1$, then the commanded speed $v_{c,i}(t)$ for the ith vehicle is the desired speed $v_{d,i}(t)$ at time t as specified by the trajectory generation algorithm. Further details on how the coordination-state rate modifies the commanded speed can be found in previous work;[12]
  - if $x_i(t) = t$, then the ith vehicle is at the position specified by the trajectory-generation algorithm t seconds after the initiation of the mission, which implies that, at time t this vehicle strictly meets its individual temporal assignment.

Given this overview of the cooperative framework, the next section introduces the formal definition of the coordination problem.

III. Problem Formulation

Consider a network of n *integrator-agents*

$$\dot{x}_i(t) = u_i(t)\,, \qquad x_i(0) = x_{i_0}\,, \qquad i \in \mathcal{I}\,, \tag{1}$$

with *dynamic information flow* $\mathcal{G}(t) := (\mathcal{V}, \mathcal{E}(t))$, where $\mathcal{V}$ and $\mathcal{E}(t)$ represent the vertices and edges of the communication graph, respectively. In our case, $\mathcal{V}$ is the group of UxSs that participate in the coordinated mission, while $\mathcal{E}(t)$ represents the communication links that are established among vehicles at each moment in time. In the above formulation, $u_i(t) \in \mathbb{R}$ is the control input, and $\mathcal{I}$ is the set of unique identification numbers of the UxSs in the fleet.

To enforce temporal constraints on the group of UxSs, we utilize the *reference agent* introduced in earlier publications.[14] This agent does not attempt coordination with any fleet member, but determines the *reference rate* $\dot{x}_R(t)$ or desired rate of the mission. The reference rate is defined such that if the mission evolves as initially programmed during the mission planning phase,[23] then

$$\dot{x}_R(t) = 1\,, \qquad x_R(0) = 0\,, \qquad \forall t \geq 0\,, \tag{2}$$

where $x_R(t) \in \mathbb{R}$ is the *reference state*. Occasionally, the dynamics of the reference rate can be modified on the fly to speed up or slow down the progress of the mission, and adapt to possible unplanned scenarios. To this end, we introduce a finite number of *rescheduling events* n_s, the corresponding rescheduling times $t_{s,i}$, and constant parameters $\gamma_{s,i}$, with $i \in \{0, 1, \ldots, n_s\}$. Then, the dynamics of the reference rate can be expressed as

$$\dot{x}_R(t) = \gamma_{s,i}\,, \qquad x_R(0) = 0\,, \qquad t_{s,i} \leq t < t_{s,i+1}\,, \qquad i \in \{0, \ldots, n_s - 1\}\,, \tag{3}$$

where $t_{s,0} = 0$, $\gamma_{s,0} = 1$, and $\dot{x}_R(t) = \gamma_{s,n_s}$ for all $t \geq t_{s,n_s}$. This is summarized in the following assumption:

Assumption 1 *The reference rate $\dot{x}_R(t)$ is a step function on $\mathbb{R}$.*[25]

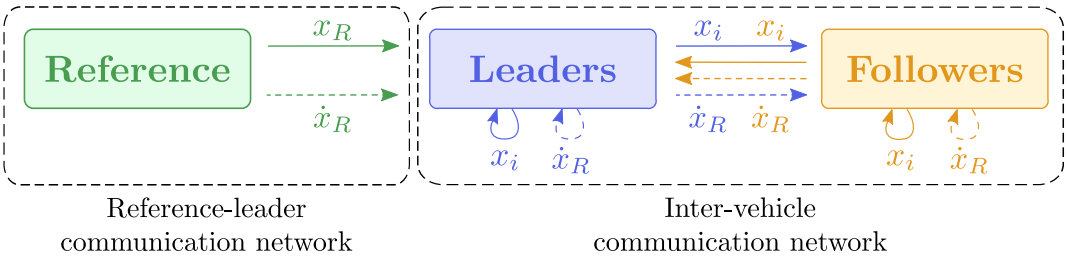

Figure 1: Communication networks, vehicle hierarchy, and flow of information.

At this point, we introduce the vehicle hierarchy and associated restrictions on the flow of information, outlined in Figure 1. Observe that this schematic introduces the reference-leader and inter-vehicle communication networks. Continuous arrows correspond with variables that are shared continuously over the network, whereas dashed arrows are associated with parameters that need only be exchanged for a limited amount of time after a rescheduling event occurs. Figure 1 classifies the fleet members in three different categories based on their role in the coordination problem and communication capabilities.

- The **reference agent** runs as a completely independent member and thus, does not require information from other vehicles. The role of the reference agent is to provide the fleet with the necessary information to enforce temporal constraints. Note that this agent continuously shares the reference state with the leaders, whereas it only sends updates on the reference rate after a rescheduling event occurs. The reference agent can be a physical or a virtual entity, running in a supervisory control facility such as mission control, or onboard the leaders.

- **Leaders** have direct access to the data from the reference agent, and communicate with other leaders and followers. In fact, leaders exchange their coordination states with other vehicles to achieve coordination. Additionally, each leader can transmit the reference rate to other leaders and followers through a multi-hoop communication protocol. Without loss of generality, vehicles with identification numbers 1 through n_ℓ are designated as fleet leaders. Hereafter, the set of all leaders will be referred to as $\mathcal{I}_\ell := \{1, \ldots, n_\ell\}$.

- **Followers** do not have direct communication capabilities with the reference agent. However, each follower shares its coordination state with other followers and leaders. Additionally, upon reception of $\dot{x}_R(t)$ they can relay this information to other vehicles through a multi-hoop communication protocol. Vehicles with identification numbers $n_\ell + 1$ through n are designated as followers. Hereafter, the set of all followers will be referred to as $\mathcal{I}_f := \{n_\ell + 1, \ldots, n\}$.

These restrictions on the flow of information aim to capture a rather general scenario, where data from the reference agent may not be available to some UxSs. This can occur when some UxSs have limited long-range communications capabilities, or when operations take place in partially shadowed areas. For instance, low-level flights where line-of-sight communications are only available to some of the UxSs. These restrictions are the reason behind the two distinct communication networks illustrated in Figure 1. For the sake of generality, we do not wish to impose any specific structure on the topology of the networks, or assume any apriori knowledge about the amount of data exchanged among group members. Accordingly, the *reference-leader communication network* satisfies the following general assumptions:

Assumption 2 *The reference agent can only exchange information with a time-varying set of leaders, denoted here by* $\mathcal{N}_R(t) \subseteq \mathcal{I}_\ell$.

Assumption 3 *Communications are unidirectional and, for simplicity,* $x_R(t)$ *is transmitted continuously and with no delays from the reference agent to the leaders.*

Assumption 4 *The connectivity of the reference-leader communication network topology satisfies the persistency of excitation (PE)-like condition*[26]

$$\min_{i \in \mathcal{I}_\ell} \left(\frac{1}{T_R} \int_t^{t+T_R} \ell_{R_i}(\tau)\, d\tau \right) \geq \mu_R\, \mathbb{I}_{\mathbf{n-1}}\,, \quad \forall\, t \geq T_R\,, \tag{4}$$

where $\ell_{R_i}(t) = 1$ if $i \in \mathcal{N}_R(t)$, and $\ell_{R_i}(t) = 0$ otherwise. Parameters $T_R > 0$ and $\mu_R \in (0, 1]$ characterize the quality of service (QoS) of the reference-leader communication network.

Assumption 5 *The reference agent transmits $\dot{x}_R(t)$ continuously, with no delays, and for a limited period of time T_R after each rescheduling event.*

Given the QoS of the reference-leader communication network specified in Assumption 4, Assumption 5 guarantees that all leaders receive the updated value of the reference rate after a rescheduling event. Similarly, the *inter-vehicle communication network* satisfies the following assumptions:

Assumption 6 *The ith vehicle can only exchange information with a time-varying set of vehicles, denoted here by $\mathcal{N}_i(t) \subset \mathcal{I}$, $i \in \mathcal{I}$.*

Assumption 7 *Communications among vehicles are bidirectional and, for simplicity, $x_i(t)$ is transmitted continuously and with no delays, $i \in \mathcal{I}$.*

Assumption 8 *The connectivity of the graph $\mathcal{G}(t)$ that models the inter-vehicle communication network topology satisfies the PE-like condition*[26]

$$\frac{1}{n}\frac{1}{T}\int_t^{t+T} \mathbf{Q}\mathbf{L}(\tau)\,\mathbf{Q}^\top d\tau \geq \mu\,\mathbb{I}_{\mathbf{n-1}}\,, \quad \forall\, t \geq T\,, \tag{5}$$

where $\mathbf{L}(t) \in \mathbb{R}^{n\times n}$ is the piecewise-constant Laplacian of the graph $\mathcal{G}(t)$, and $\mathbf{Q} \in \mathbb{R}^{(n-1)\times n}$ is a matrix satisfying $\mathbf{Q1_n} = \mathbf{0}$, and $\mathbf{QQ}^\top = \mathbb{I}_{\mathbf{n-1}}$, with $\mathbf{1_n} \in \mathbb{R}^n$ being the vector whose components are all 1. Parameters $T > 0$ and $\mu \in (0, 1]$ characterize the QoS of the inter-vehicle communication network, and are an integral measure of the connectivity of graph $\mathcal{G}(t)$.

Assumption 9 *Upon reception of the updated value of $\dot{x}_R(t)$ after a rescheduling event, the ith vehicle transmits $\dot{x}_R(t)$ continuously and with no delays for a limited period of time T to other vehicles in the fleet.*

Given the QoS for the inter-vehicle communication network specified in Assumption 8, Assumption 9 guarantees that all vehicles receive the updated value of the reference rate. Considering Assumptions 1 through 9, the control objective is to design a *distributed protocol* that solves the following *consensus problem*:

$$x_i(t) - x_j(t) \overset{t\to\infty}{\longrightarrow} \left[-\tfrac{\Delta_c}{2}, \tfrac{\Delta_c}{2}\right], \qquad \forall\, i, j \in \mathcal{I}\,, \tag{6a}$$

$$x_i(t) - x_R(t) \overset{t\to\infty}{\longrightarrow} \left[-\tfrac{\Delta_a}{2}, \tfrac{\Delta_a}{2}\right], \qquad \forall\, i \in \mathcal{I}_\ell\,, \tag{6b}$$

$$\dot{x}_i(t) - \dot{x}_R(t) \overset{t\to\infty}{\longrightarrow} 0\,, \qquad \forall\, i \in \mathcal{I}\,, \tag{6c}$$

where $\Delta_c, \Delta_a \geq 0$ are the width of the coordination window and the arrival window, respectively. Equation (6a) enforces the coordination constraints among the UxSs in the fleet. The leftmost term represents the inter-vehicle coordination error (ICE). Equation (6b) imposes temporal specifications on the leaders. In this case, the leftmost term represents the vehicle temporal error (VTE). Finally, Equation (6c) ensures that the mission develops at the desired rate. The leftmost term in this equation is the vehicle rate error (VRE). The next section provides a deeper insight into Equation(6) through a simple example.

A. Physical Interpretation of the Consensus Problem

Figure 2 provides a particular representation of the consensus problem defined in Equation (6). For illustrative purposes, Figure 2 shows a formation pattern for a fleet of three vehicles, the reference agent, the leader, and the follower, along with their corresponding paths depicted by dashed blue lines. All the vehicles are moving rightward, and the faded circles represent the position of the vehicles in past instances. In this particular scenario the reference agent is a real vehicle and not a virtual entity. Note, however, that this cooperative framework[12] does not necessarily lead to swarming behaviors.

Since the reference agent runs independently of all other vehicles, the time evolution along its path is exclusively determined by the reference rate $\dot{x}_R(t)$ and the desired speed profile $v_{d,R}(t)$, computed during the trajectory generation phase.[23] As a result, each point along the path of the reference agent has a fixed temporal specification, as highlighted in Figure 2. It is remarked that $\dot{x}_R(t) = 1$ or $\dot{x}_i(t) = 1$ for all t does

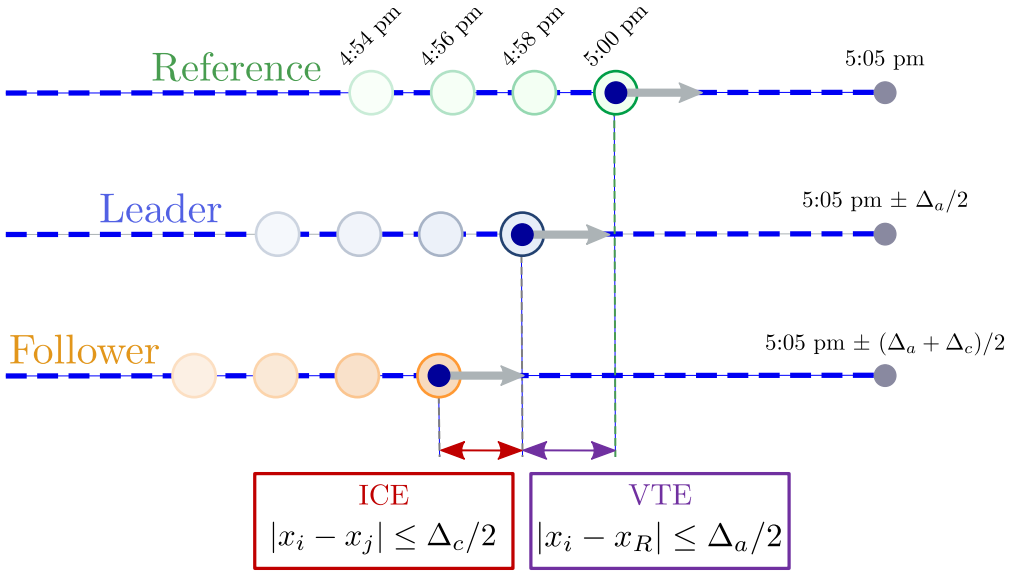

Figure 2: Illustrative example of the consensus problem.

not imply that the speed profile of the corresponding vehicle is constant. In fact, it indicates that the UxS in question is commanded to strictly follow the desired speed profile as computed in the trajectory generation phase. Now, let us assume that after a rescheduling event the reference rate is set to $\dot{x}_R(t) = 1.2$. In this case, the mission would evolve 20% faster than initially planned. Accordingly, the commanded speed will be the desired speed profile scaled by 1.2.

The end-time specifications for the vehicles are shown above the gray circles that mark the end of each path. Again, for illustrative purposes, the nominal time of arrival to the final destination is 5:05 pm for all vehicles. However, this cooperative framework allows the specification of different arrival times for each of the vehicles. Further details on how to impose sequential arrival times are described in previous work.[24] It is also noted that this framework allows the specification of intermediate and end-time temporal constraints, which can be of interest in multi-objective missions.

Contrary to the reference agent, the leader and the follower depicted in Figure 2 exploit the information shared over the networks to achieve coordination and satisfy their temporal constraints. Note that these UxSs have, to some extent, a degree of freedom to move around a bounded neighborhood of the reference agent, defined by Δ_c and Δ_a. From Figure 2, it becomes clear that Δ_c is a temporal measure of the allowable discoordination among all the vehicles in $\mathcal{I}$, while Δ_a is the leeway given to the leaders to satisfy their temporal specifications. Additionally, it can be inferred from Figure 2 that temporal constrains are not necessarily the same for the leaders and the followers. In fact, Equations (6a) and (6b) lead to

$$x_i(t) - x_R(t) \quad \overset{t\to\infty}{\longrightarrow} \quad \left[-\tfrac{\Delta_a+\Delta_c}{2}, \tfrac{\Delta_a+\Delta_c}{2}\right], \qquad \forall\, i \in \mathcal{I}_f\,. \tag{7}$$

Since followers have no knowledge of the reference state, see Figure 1, they learn their temporal specifications through coordination with the leaders. As a result, the margin of error on the temporal specifications of the followers also depends on the width of the coordination window Δ_c. This provides the opportunity to impose a dual behavior on the temporal constraints using the vehicle hierarchy. This can be advantageous in some mission scenarios, as illustrated in the next section.

IV. Time-Coordination Strategies

In this section, the possible values of Δ_c and Δ_a are utilized to define several types of coordination and temporal constraints. To emphasize the usability of the resulting time-coordination strategies, we provide real-world examples where these strategies can be used to automate procedures that are often controlled by human operators. Depending on the value of the coordination window Δ_c, we define the following coordination types:

- **Tight coordination** ($\Delta_c = 0$) forces the vehicles to strictly observe their coordination constraints, and drives the ICE to zero; see Equation (6a). This type of coordination is typical of scenarios where maintaining the desired relative position among vehicles is crucial; see examples depicted in Figures 3a, 4a, and 5a. Tight coordination can be used as a tool to ensure vehicles do not violate the minimum safety distance separation when assigned time-deconflicted trajectories.

- **Loose coordination** ($\Delta_c > 0$) defines an allowable margin of error in the coordination among vehicles, and ensures that the ICE converges to a $\Delta_c/2$-neighborhood of zero; see Equation (6a). Naturally, loose coordination is a relaxation of tight coordination specifications. Loose coordination constraints are common in mission scenarios where coordination is still utilized to ensure inter-vehicle separation. However, in this case time-deconflicted trajectories must be computed such that a bounded error in the coordination among vehicles does not jeopardize the integrity of the UxSs; see examples shown in Figures 3b, 4b, and 5b.

Similarly, based on the possible values of the arrival window Δ_a, we define the following types of temporal constraints:

- **Unenforced temporal constraints** (Δ_a undefined) do not impose any temporal specifications on the UxSs. Since Δ_a is undefined, Equations (6b) and (7) are not defined either. Note that, in this case, the function of the reference agent is limited to determining the rate of the mission. Thus, the reference agent does not need to share its state with the leaders in the fleet. This type of temporal constraint is used in missions that do not require the specification of an arrival time or arrival window at any point along the path of the vehicles. In scenarios with unenforced temporal constraints, the reference agent is typically not a member of the fleet, but a supervisory control facility that dictates the pace of the mission. Two examples that illustrate the use of unenforced temporal constraints are depicted in Figure 3.

(a) Coordinated maneuvers at an airshow, tight coordination (Image is courtesy of U.S. Navy Blue Angels).

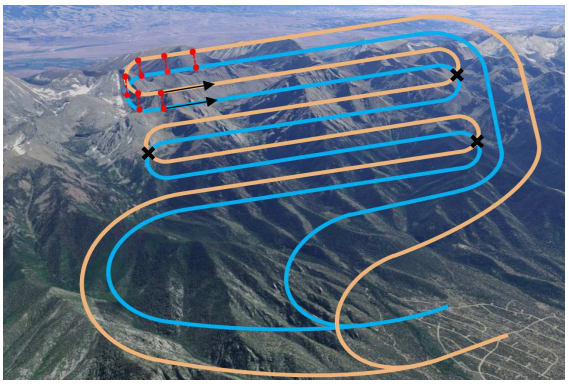

(b) Coordinated search and rescue operation, loose coordination.

Figure 3: Mission scenarios with unenforced temporal constraints.

Figure 3a presents a scenario that combines tight coordination with unenforced temporal constraints. Coordinated maneuvers performed by the US Navy Blue Angels resulting in a specific flight formation pattern are shown in this figure. This type of exercise requires that the aircraft meet desired relative position specifications with extreme precision due to the close proximity among aircraft. This can be translated into our framework as tight coordination. Note also that the vehicles depicted in Figure 3a are not subject to temporal specifications, since the aircraft are not required to arrive to any specific location at any specific time. Consequently, this particular scenario could be automated using tight coordination and unenforced temporal constraints.

Figure 3b depicts a coordinated search and rescue operation in a difficult-access mountainous area. The trajectories in blue and orange show two UAVs take off, fly a Boustrophedon-like pattern, and land at the base of the mountain. The red dots indicate the location of the UAVs at different instances. In this case, cooperation among vehicles is leveraged to cover a larger area in a smaller amount of time. This

is of especial importance in life-threatening scenarios, where prompt assessment and localization of victims significantly increases survival rates. Note that the trajectories are not spatially deconflicted, since the paths overlap at the points marked by a black cross. Therefore, in the absence of coordination the vehicles may collide in flight at these points. Lack of coordination is especially dangerous in the presence of external disturbances that may affect the progress of the UAVs along their assigned trajectories differently. One example of such exogenous disturbances are wind gusts. Moreover, it is often desired that the sensing regions of the vehicles slightly overlap, which also requires some sort of coordination. Notice, however, that tight coordination is not necessary since the vehicles can deviate along their nominal trajectories, to some extent, without the risk of collision. Again, this scenario does not impose any temporal specifications on the UAVs since they are not required to fly above any particular point at a specific time. As a result, this mission could be implemented using loose coordination and unenforced temporal constraints. More importantly, with the adequate sensing payload, this type of missions could be automated and performed at night, when conventional manned search and rescue operations often need to halt.

- **Strict temporal constraints** ($\Delta_a = 0$) force the leaders to precisely observe their temporal specifications, see Equation (6b). This type of constraint is characteristic of missions that require the UxSs to be at one or more specific points along their paths at a particular moment in time. Again, two scenarios that illustrate the use of strict temporal constraints in real-world applications are shown in Figure 4.

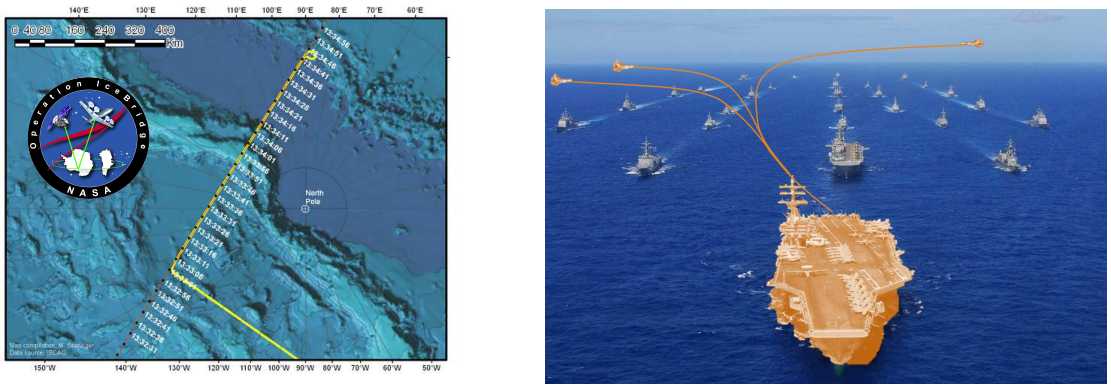

(a) Validation and calibration of satellite data, tight coordination (Image is courtesy of Michael Studinger,[27] adapted by Javier Puig-Navarro).

(b) Coordinated sea-air maneuvers, loose coordination (Image is courtesy of U.S. Navy, by Dylan McCord, adapted by Javier Puig-Navarro).

Figure 4: Mission scenarios with strict temporal constraints.

Calibration and validation of satellite data is a representative example that combines tight coordination with strict temporal constraints. In such experiments, one or more aircraft are tasked to fly cooperatively to collect data that will later be compared to the information obtained by the satellite. Often, the satellite over-pass and the aircraft measurements must take place simultaneously, since the variables measured (temperature, humidity, ice thickness, concentration of specific pollutants...) may vary with time. Due to the cost and complexity of orbital maneuvers, the satellite does not attempt coordination with the fleet of aircraft and acts as the reference agent. Conversely, aircraft coordinate with each other and attempt to meet the temporal and spatial specifications determined by the satellite's orbit. One example of such missions is NASA's IceBridge program,[27] which performed low-altitude flights to calibrate the radar altimeter onboard the CryoSat-2, a European Space Agency (ESA) environmental research satellite. Figure 4a shows the coordinated trajectories of a DC-8 in yellow, and the CryoSat-2 in orange, along with the times of the satellite over-pass. In this case, the aircraft and the satellite had to be both spatially and temporally coordinated to achieve the desired calibration accuracy, and avoid measurement bias due to the drifting of the sea ice pack.

Figure 4b shows a fleet of vessels engaged in coordinated maneuvers. Meanwhile, three aircraft are tasked to land on the runway of the aircraft carrier, highlighted in orange. Note that the vessels do not

require tight coordination among themselves. Since the vessels are quite apart, small deviations in their formation will not lead to collision. On the other hand, the aircraft must precisely meet the spatial and temporal specifications defined by the aircraft carrier. Since the carrier is the largest and most expensive vehicle to operate, it behaves as the reference agent. In order to achieve the aforementioned collective behavior, the aircraft are elected as leaders, the remaining vessels are the followers, and loose coordination with strict temporal constraints is the time-coordination strategy of choice.

- **Relaxed temporal constraints** ($\Delta_a > 0$) provide the leaders and consequently the followers, see Equations(6b) and (7), with an allowable margin of error in their temporal specifications. Relaxed temporal constraints must be imposed in missions that require the vehicles to reach one or more points along their paths within a temporal window. Figure 5 presents two scenarios where relaxed temporal constraints are necessary to automate the mission.

(a) Coordinated aerial refueling, tight coordination (Image is courtesy of U.S. Air Force, by Suzanne M. Jenkins).

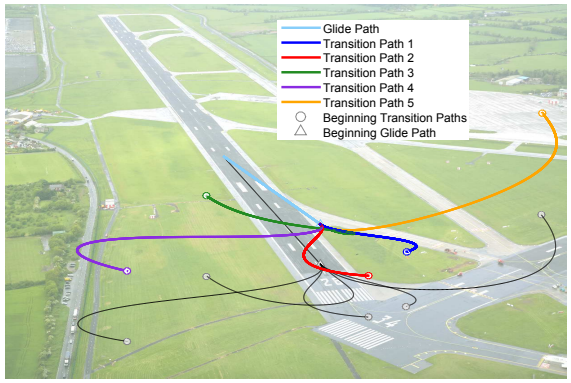

(b) Coordinated auto-landing scenario, loose coordination.

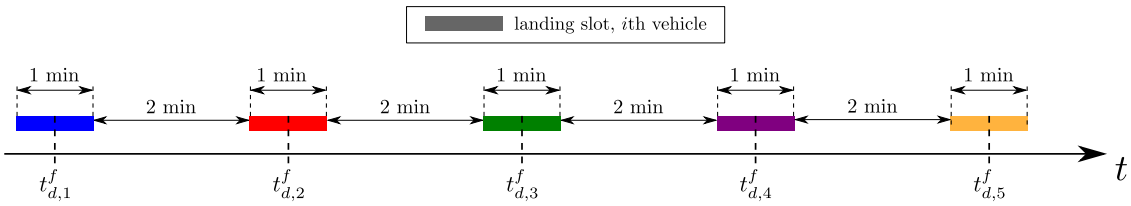

(c) Assigned landing slots for the five UAVs in the coordinated auto-landing scenario.

Figure 5: Mission scenarios with relaxed temporal constraints.

Figure 5a shows a coordinated aerial refueling maneuver involving two Tornado GR4 and a Boeing KC-135R Stratotanker. Generally, a refueling exercise is not the end goal of a mission, but it is often a needed intermediate phase. Let us assume that the two GR4 Tornado are tasked to arrive to their final destination within an arrival window. Due to the close proximity nature of aerial refueling operations, the tanker and the two Tornado need to satisfy very precise relative position constraints. Additionally, these aircraft must arrive to their final destination within a pre-defined temporal slot. As a result, this scenario could be automated using tight coordination, and relaxed temporal constraints.

Figure 5b depicts an auto-landing scenario involving five UAVs. Each vehicle is requested to follow its assigned trajectory and land on the runway within a predefined arrival window. Figure 5c shows the nominal arrival time $t^f_{d,i}$ and desired arrival window for each of the vehicles. The UAVs can arrive at any time within the assigned landing slot. Note also that the spacing of the landing slots guarantees that the vehicles will land at least two minutes apart. Furthermore, the trajectories assigned to the UAVs are time-deconflicted. Consequently, the vehicles must coordinate to ensure safe inter-vehicle separation. Thereby, this auto-landing scenario could be implemented using loose coordination and relaxed temporal constraints.

The combination of coordination constraints and temporal specifications introduced above defines six

Table 1: Time-coordination strategies.

		Coordination	
		Tight	Loose
Temporal constraints	Unenforced	$-\quad, \Delta_c = 0$	$-\quad, \Delta_c > 0$
	Strict	$\Delta_a = 0\,,\ \Delta_c = 0$	$\Delta_a = 0\,,\ \Delta_c > 0$
	Relaxed	$\Delta_a > 0\,,\ \Delta_c = 0$	$\Delta_a > 0\,,\ \Delta_c > 0$

different time-coordination strategies, summarized in Table 1. Nonetheless, there exist scenarios with coordination and temporal requirements that cannot be captured by the time-coordination strategies presented so far. Consider, as an example, a slight modification of the mission shown in Figure 4b. Figure 6 shows the same fleet of vessels engaged in coordinated maneuvers. However, now three aircraft are tasked to land on the aircraft carrier highlighted in orange, while other three aircraft have to land on the carrier highlighted in green. One option would be to maintain loose coordination with strict temporal constraints, create a virtual reference agent, and elect the two carriers and six aircraft as leaders. While this may solve the problem, the degree of freedom that allowed a bounded discoordination between carriers has been eliminated. Moreover, this would force all aircraft to precisely coordinate with each other, which is also unnecessary. As a result, the fleet would be over-constrained, leading possibly to larger control inputs, larger speed corrections, and hence higher fuel consumption. If one wishes to allow bounded disagreement on the coordination states of the carriers and between orange and green aircraft, the only solution is to define agent-specific coordination behaviors. However, this type of coordination problem cannot be formulated as in Equation 6. Consequently, the development of control laws for agent-specific coordination behaviors is beyond the scope of this paper. In the next section, distributed control laws for the time-coordination strategies contained in Table 1 are presented.

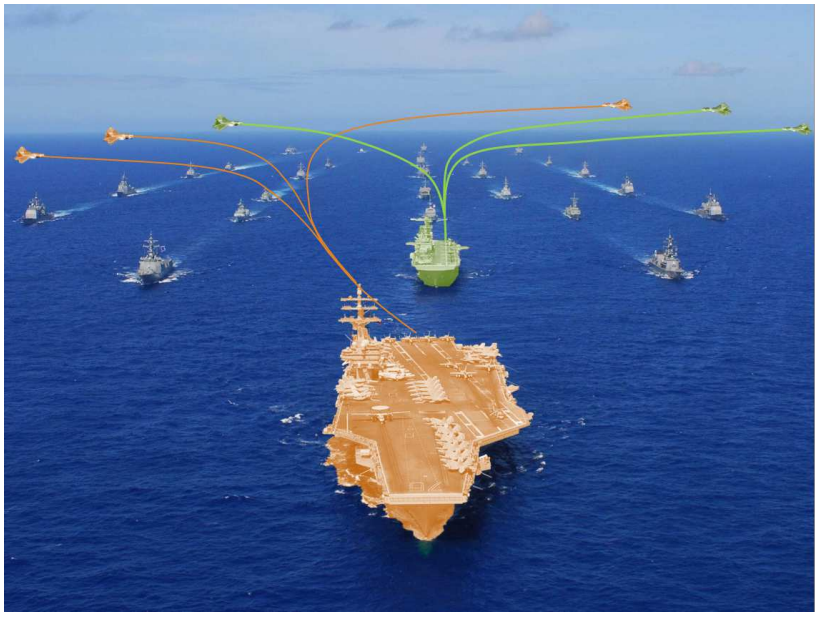

Figure 6: Mission scenario with agent-specific coordination constraints (Image is courtesy of U.S. Navy, by Dylan McCord, adapted by Javier Puig-Navarro).

V. Distributed Control Law

To solve the consensus problem defined in Equation (6), we propose the following distributed coordination control law:

$$\text{Leaders} \begin{cases} u_i(t) &= -k_P \sum_{j\in\mathcal{N}_i} \omega_{c_{i,j}}(x_i - x_j) - k_{P_R}\,\omega_{R_i}\,\ell_{R_i}(x_i - x_R) + \chi_i \\ \dot{\chi}_i(t) &= -k_I \sum_{j\in\mathcal{N}_i} \omega_{c_{i,j}}(x_i - x_j) - k_{I_R}\,\omega_{R_i}\,\ell_{R_i}(x_i - x_R) + \alpha_i(\dot{x}_R - \chi_i) \\ \chi_i(0) &= \chi_{i_0} \end{cases} , \quad i \in \mathcal{I}_\ell \tag{8a}$$

$$\text{Followers} \begin{cases} u_i(t) &= -k_P \sum_{j\in\mathcal{N}_i} \omega_{c_{i,j}}(x_i - x_j) + \chi_i \\ \dot{\chi}_i(t) &= -k_I \sum_{j\in\mathcal{N}_i} \omega_{c_{i,j}}(x_i - x_j) + \alpha_i(\dot{x}_R - \chi_i) \\ \chi_i(0) &= \chi_{i_0} \end{cases} , \quad i \in \mathcal{I}_f \tag{8b}$$

where $k_P, k_I, k_{P_R}, k_{I_R} > 0$ are control gains; $\omega_{c_{i,j}}(t)$ is the *coordination link weight* associated with vehicles i and j; $\omega_{R_i}(t)$ is the *reference link weight* of the ith leader; $\alpha_i(t) = 1$ if $\dot{x}_R(t)$ is available to the ith UxS, $\alpha_i(t) = 0$ otherwise; and $\chi_i(t) \in \mathbb{R}$ is the *integral state* of the ith fleet member. The distributed coordination control law has a proportional integral structure that provides both, leaders and followers, with disturbance rejection capabilities. The main difference between the coordination control law for the leaders and the followers is the use of the reference state. Notice that leaders use the reference state to enforce temporal constraints whenever it is available through the network, namely $\ell_{R_i}(t) = 1$; while followers cannot use this information, as illustrated in Figure 1. Next, the role of the three basic terms that can be observed in Equation (8) is detailed:

- Terms that include the coordination link weight $\omega_{c_{i,j}}(t)$ enforce coordination among vehicles.
- Terms that incorporate the reference link weight $\omega_{R_i}(t)$ impose temporal constraints on the leaders. Note that this term is not present in the control law of the followers. Consequently, followers learn their temporal specifications through coordination with the leaders, as previously inferred from Equation (7).
- Terms that contain $\dot{x}_R(t)$ help UxSs learn the desired rate of the mission. In the case of tight coordination, convergence can be achieved even if $\alpha_i(t) = 0$ for all $i \in \mathcal{I}_f$ and all t. This occurs because the integral term in the control law allows the followers to learn a new reference rate from the leaders. Notice that the availability of the reference rate $\dot{x}_R(t)$ in Equation (8b), namely $\alpha_i(t) = 1$, improves convergence of the integral state of the followers to the desired rate of the mission.

Recall that Equation (8) is the proposed solution for all the time-coordination strategies defined in Section IV. Next, we define the link weight decision logic for each of the time-coordination strategies in Table 1.

A. Link Weight Decision Logic

The decision logic for the coordination link weights $\omega_{c_{i,j}}(t)$ defines the type of coordination constraints enforced on the UxSs. Table 2 contains the decision logic for tight and loose coordination. From Equation (8), we know $\omega_{c_{i,j}}(t)$ is not used if $j \notin \mathcal{N}_i(t)$. Therefore, in such instances the value of $\omega_{c_{i,j}}(t)$ does not need to be specified. Notice in Table 2 that for tight coordination the ith vehicle always "listens" to the jth UxS if the coordination state of the latter is available through the network. However, for loose coordination the ith vehicle only "listens" to the jth UxSs if the coordination state of the latter is available through the network, and the ICE lies outside the coordination window, specified by Δ_c. In order to avoid chattering, the decision logic for loose coordination is also subject to slow switching constraints. To this end, we define the switching times $t_{c_{i,j,1}}$,$t_{c_{i,j,2}}$,... and delay the switching of $\omega_{c_{i,j}}(t)$, defined in Table 2, until the following inequality is met:

$$t_{c_{i,j,k+1}} - t_{c_{i,j,k}} \geq \tau_{d_c}\,, \qquad \forall k \in \mathbb{N}\,,$$

where τ_{d_c} is the dwell time for the coordination link weights. Furthermore, it is expected that these slow switching constraints are required to prove stability of the control law for loose coordination.

Similarly, the decision logic for the reference link weights $\omega_{R_i}(t)$ defines the type of temporal constraints imposed on the fleet. Table 3 contains the decision logic for unenforced, strict, and relaxed temporal

Table 2: Decision logic for the coordination link weights.

Tight	Loose
$\omega_{c_{i,j}}(t) = 1$	$\omega_{c_{i,j}}(t) = \begin{cases} 1\,, & \lvert x_i(t) - x_j(t)\rvert \geq \Delta_c/2 \\ 0\,, & \lvert x_i(t) - x_j(t)\rvert < \Delta_c/2 \end{cases}$

specifications. As shown in Equation (8), $\omega_{R_i}(t)$ is not utilized if $\ell_{R_i}(t) = 0$, or equivalently $i \notin \mathcal{N}_R(t)$. Consequently, the value of $\omega_{R_i}(t)$ does not need to be defined in such instances. According to Table 3, for unenforced temporal constraints, leaders never "listen" to the reference state. Conversely, for strict temporal constraints leaders always "listen" to the reference state, if available through the reference-leader communication network. Finally, for relaxed temporal specifications, leaders only "listen" to the reference state if available through the network and the VTE lies outside the arrival window, defined by Δ_a. Again, to avoid chattering the decision logic for relaxed temporal specifications is subject to slow switching constraints. To this purpose, we define the switching times $t_{R_{i,1}}$,$t_{R_{i,2}}$,... and delay the switching of $\omega_{R_i}(t)$ until the following inequality is met:

$$t_{R_{i,k+1}} - t_{R_{i,k}} \geq \tau_{d_R}\,, \qquad \forall k \in \mathbb{N}\,,$$

where τ_{d_R} is the dwell time for the reference link weights. As before, it is expected that these slow switching constraints are required to prove stability of the control law for relaxed temporal specifications.

Table 3: Decision logic for the reference link weights.

Unenforced	Strict	Relaxed
$\omega_{R_i}(t) = 0$	$\omega_{R_i}(t) = 1$	$\omega_{R_i}(t) = \begin{cases} 1\,, & \lvert x_i(t) - x_R(t)\rvert \geq \Delta_a/2 \\ 0\,, & \lvert x_i(t) - x_R(t)\rvert < \Delta_a/2 \end{cases}$

Next, simulation results for all the possible combinations of the decision logic described in Tables 2 and 3 are provided.

VI. Simulation Scenarios

To demonstrate the efficacy of the control law proposed in Equation (8), simulation results for the six time-coordination strategies are presented. All the simulation scenarios were run for a fleet of $n = 5$ vehicles with the same initial conditions, reference-leader network topology, and inter-vehicle network topology. Vehicles 1 and 2 were designated as leaders. The initial conditions for the coordination states $x_i(t)$ were randomly picked from a ball in $\mathbb{R}^n$ of radius $r_x = \|\mathbf{x_0}\|_2 = 10\ s$ centered at the origin, and with uniform probability distribution, where $\mathbf{x_0} := [x_{1_0}, x_{2_0}, x_{3_0}, x_{4_0}, x_{5_0}]^\top$. The initial values for the coordination states were

$$\mathbf{x_0} = [\ -0.21\ ,\ 3.58\ ,\ 6.59\ ,\ 0.00\ ,\ -2.86\ ]^\top .$$

Similarly, initial conditions for the integral states $\chi_i(t)$ were randomly picked from a ball in $\mathbb{R}^n$ of radius $r_\chi = \|\chi_\mathbf{0}\|_2 = 0.30\ s/s$ centered at $\mathbf{1_n}$, and with uniform probability distribution, where $\chi_\mathbf{0} := [\chi_{1_0}, \chi_{2_0}, \chi_{3_0}, \chi_{4_0}, \chi_{5_0}]^\top$. The initial values for the integral states were

$$\chi_\mathbf{0} = [\ 0.79\ ,\ 1.15\ ,\ 0.98\ ,\ 1.01\ ,\ 0.92\ ]^\top .$$

For the first 30 s of the simulation, the reference rate was set to the nominal value. After the rescheduling event occurs at $t = 30\ s$, the reference rate was set to 1.2 s/s

$$\dot{x}_R(t) = \begin{cases} 1\,, & 0 \leq t < 30 \\ 1.2\,, & t \geq 30 \end{cases} .$$

The inter-vehicle time-varying network topology was generated using a pseudo-random network generator that lets the user specify upper and lower bounds on the connectivity of the network $\hat{\mu}_{\min} \leq \hat{\mu}(t) \leq \hat{\mu}_{\max}$ for

a given T, where $\hat{\mu}(t)$ is defined as follows:

$$\hat{\mu}(t) := \frac{1}{n}\frac{1}{T}\int_{t-T}^{t} \mathbf{QL}\,(\tau)\,\mathbf{Q}^{\top}\,d\tau\,, \qquad \forall t \geq T\,.$$

The parameters that control the QoS of the inter-vehicle communication network were set to the following values:

$$\hat{\mu}_{\min} = 0.25\,, \qquad \hat{\mu}_{\max} = 0.40\,, \qquad T = 5.00\ s\,.$$

The reference-leader communication network topology was generated using a modification of the pseudo-random network topology generator. This algorithm lets the user specify upper and lower bounds on the connectivity of the network for each of the leaders $\hat{\mu}_{R,i_{\min}} \leq \hat{\mu}_{R,i}(t) \leq \hat{\mu}_{R,i_{\max}}$ for a given T_R, where $i \in \mathcal{I}_\ell$ and $\hat{\mu}_{R,i}(t)$ is defined as follows:

$$\hat{\mu}_{R,i}(t) := \frac{1}{T_R}\int_{t-T_R}^{t} \ell_{R_i}(\tau)\,d\tau\,, \qquad \forall t \geq T_R\,, \qquad i \in \mathcal{I}_\ell.$$

The parameters that specify the QoS of the leader-reference communication network were set to the following values:

$$\hat{\mu}_{R,i_{\min}} = 0.30\,, \qquad \hat{\mu}_{R,i_{\max}} = 1.00\,, \qquad T_R = 5.00\ s\,, \qquad \forall i \in \mathcal{I}_\ell.$$

Figures 7a and 7b show the connectivity of the inter-vehicle and the reference-leader communication networks, respectively. Recall Assumptions 4 and 8, and note that for the simulation scenarios presented $\mu = 0.27$ and $\mu_R = 0.3$.

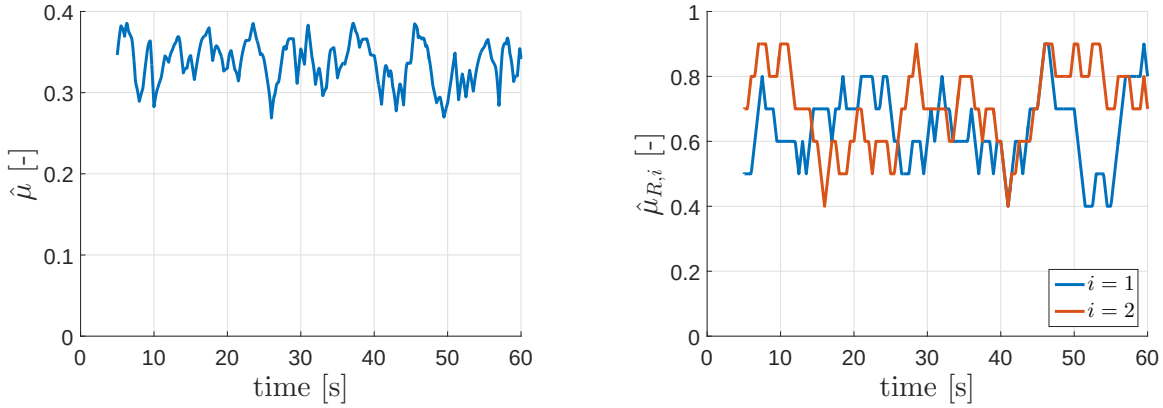

(a) Inter-vehicle communication network.

(b) Reference-leader communication network.

Figure 7: Connectivity.

The values chosen for the control gains were

$$k_P = 0.20\,, \qquad k_I = 0.02\,, \qquad k_{P_R} = 0.20\,, \qquad k_{I_R} = 0.02\,.$$

The width of the coordination window, the arrival window, and the dwell times for the link weights were set to

$$\Delta_c = 4.00\ s\,, \qquad \Delta_a = 2.00\ s\,, \qquad \tau_{d_c} = 1.00\ s\,, \qquad \tau_{d_R} = 1.00\ s\,.$$

Figure 9 shows the simulation results for unenforced temporal specifications with both tight and loose coordination constraints. Notice that for tight coordination the ICE converges to the origin; see Figure 9a. However, for loose coordination the ICE converges to a $\Delta_c/2$-neighborhood of the origin; see Figure 9b. The black dashed lines in Figures 9a and 9b indicate the control objective for the ICE. Observe that for tight coordination the control objective is depicted by a single line; whereas for loose coordination it is represented by two dashed lines, and anything that falls between them meets the coordination specifications. Note also that convergence to the desired set occurs significantly faster for loose coordination since the fleet is asked for a smaller control effort. Figures 9c and 9d show the VTE for tight and loose coordination,

respectively. It can be observed that the VTE of all the vehicles converges to a single bounded value in Figure 9c; while in Figure 9d the VTE of each vehicle stabilizes at different values. Notice that Figures 9c and 9d do not include any dashed black lines, indicating that there are no control objectives defined in terms of the VTE, as expected of unenforced temporal constraints. Figures 9e and 9f show the time evolution of the integral states for tight and loose coordination, respectively. In both cases, the integral states converge to the reference rate, even after the rescheduling event. Figures 9g and 9h depict the control inputs associated with the aforementioned coordination strategies. The non-smooth nature of the control input is the result of the switching inter-vehicle and reference-leader network topologies. For loose coordination in Figure 9h, the switching of the coordination link weights also contributes to the non-smoothness of the control input. There exist several techniques suitable to reduced this type of effects. In particular, the development of estimators that provide useful information about the coordination state of other vehicles can be used to smoothen the control input, when information is not received over the network. Another, technique would be the use of continuous link weights that do not lead to hybrid system behaviors. Observe that, in general, the control input converges faster to the desired reference rate for loose coordination.

Figure 10 shows the simulation results for strict temporal specifications with both tight and loose coordination. Again, tight coordination forces all the vehicles to converge to the same coordination state, as shown in Figure 10a; whereas loose coordination allows bounded disagreement in the coordination states of all vehicles; see Figure 10b. Figures 10c and 10d show the time-evolution of the VTE. The major difference with Figures 9c and 9d is the presence of dashed black lines, indicating that temporal constraints are now being actively enforced on the vehicles. Figure 10c shows that the coordination state of all the vehicles eventually converges to the reference coordination state, as expected of tight coordination with strict temporal constraints. For loose coordination, Figure 10d provides numerical evidence that the coordination state of the two leaders converges to the reference state; while the coordination states of the followers converge to and remain in a $\Delta_a/2$-neighborhood of the reference state. This behavior was anticipated by Equations (7) and (6b). Figures 10e and 10f show the evolution of the integral states. Again, the integral states converge to the reference rate, even after the rescheduling event. Figures 10g and 10h show the time-evolution of the control input for tight and loose coordination, respectively.

Figure 11 shows the simulation results for relaxed temporal specifications with both tight and loose coordination constraints. Figures 11c and 11d show the VTE for tight and loose coordination, respectively. Note that in Figure 11c the VTE converges to the same value as time progresses due to the tight coordination constraints. Simultaneously, the VTE of all the vehicles satisfies the loose temporal specifications depicted by the two black dashed lines. Figure 11d shows four black dashed lines. The region defined by the inner lines represents the temporal specifications of the leaders; whereas, the area between the two outer lines represents the temporal specifications of the followers. This is due to the fact that followers do not have access to the reference state and learn their temporal constraints through coordination with the leaders. In this particular case, vehicle 3 converges to the region defined by the outer dashed black lines, as expected of a follower. The VTE of the remaining vehicles converges to the region defined by the inner dashed black lines. Hence, not only do the remaining followers satisfy their temporal constraints, but also the stricter temporal constraints of the leaders. Conclusions regarding the remaining subfigures are similar to the observations made for Figures 9 and 10.

The simulation results presented in Figures 9, 10, and 11 provide numerical evidence that the control law defined in Equation (8), along with the link weight decision logic in Tables 2 and 3, solve the consensus problem defined in Equation (6).

A. Importance of Selecting Appropriate Constraints

Given the control law in Equation (8) and the link weight decision logic defined in Tables 2 and 3, one may question if the complexity introduced in the system as compared to previous consensus algorithms is justifiable, especially considering that with tight coordination and strict temporal specifications all the mission examples described in Section IV could be performed safely. Note, however, that this approach will constrain the systems in unnecessary ways. To answer this fundamental question, we introduce a measure of the control effort

$$\epsilon(t) = \dot{\mathbf{x}}(t) - \dot{x}_R(t)\mathbf{1_n}\,, \tag{9}$$

where $\dot{\mathbf{x}}(t) = [\dot{x}_1(t), \ldots, \dot{x}_n(t)]^\top$. Recall that $\dot{x}_i(t)$ acts as a scaling factor of the speed profile in the cooperative path-following framework.[12] Thus, $\epsilon(t)$ is related to the speed command and fuel consumption

of the fleet of UxSs. Figure 8 shows the truncated $\mathcal{L}_2$ norm of $\epsilon(t)$ as a function of time for the six simulation scenarios represented in Figures 9, 10, and 11. The acronyms CC and TC in the legend stand for coordination constraints and temporal constraints, respectively. Notice that $\|\epsilon(t)\|_{\mathcal{L}_2}$ converges to a finite value for each of the time-coordination strategies. Observe also that the control effort for loose coordination is significantly smaller than for tight coordination. Note also that the control effort associated with unenforced temporal constraints is slightly smaller than that of relaxed temporal specifications, which at the same time is smaller than that of strict temporal constraints. Consequently, if utilized appropriately the additional complexity introduced can be leveraged to reduce the collective control effort of the fleet, leading to a reduction in fuel consumption. In summary, operators with supervisory control over the cooperative framework should avoid over-constraining the system by imposing the least restrictive coordination and temporal specifications that the mission can safely admit.

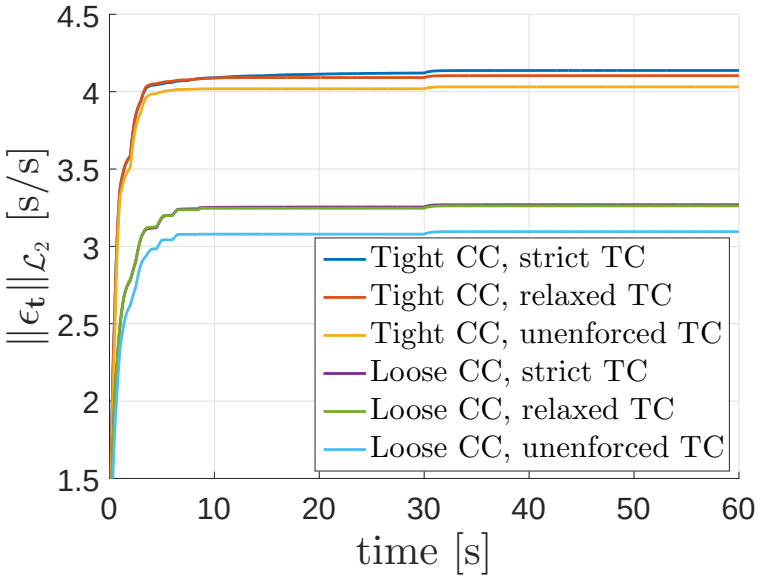

Figure 8: Truncated $\mathcal{L}_2$ norm of the control effort.

VII. Conclusions

This paper expands the spectrum of time-coordination strategies available for multi-UxSs missions. In particular, six standard time-coordination strategies that naturally result from the combination of coordination constraints and temporal specifications are proposed in this work. Real-world scenarios where each strategy can be used are discussed to show the applicability of this framework. A mission scenario that requires a coordination behavior unattainable by this framework is used to illustrate the limitations of the current set of time-coordination strategies. This example is also used to introduce agent-specific coordination constraints, which will be the object of future research. A distributed control law capable of enforcing the coordination and temporal specifications presented is formulated in this paper. The control law utilizes the decision logic of a set of link weights to define the type of coordination and temporal constraints imposed on the vehicles. Simulation results for the six time-coordination strategies provide numerical evidence of the efficacy of the proposed control law. Future efforts will include the formal derivation of conditions under which the proposed control law is stable. The analysis of the simulation results highlights the importance of imposing the least restrictive set of constraints on the vehicles. By doing so, the collective control effort will be reduced, leading to a decrease in fuel consumption.

References

[1]Cokelet, E. D., Meinig, C., Lawrence-Slavas, N., Stabeno, P. J., Mordy, C. W., Tabisola, H. M., Jenkins, R., and Cross, J. N., "The Use of Saildrones to Examine Spring Conditions in the Bering Sea," *Oceans*, Washington, DC, October 2015, pp. 1–7.

[2]Durban, J. W., Moore, M. J., Chiang, G., Hickmott, L. S., Bocconcelli, A., Howes, G., Bahamonde, P. A., Perryman, W. L., and LeRoi, D. J., "Photogrammetry of Blue Whales with an Unmanned Hexacopter," *Marine Mammal Science*, Vol. 32, No. 4, October 2016, pp. 1510–1515.

[3]Samiappan, S., Turnage, G., Hathcock, L., Casagrande, L., Stinson, P., and Moorhead, R., "Using Unmanned Aerial Vehicles for High-resolution Remote Sensing to Map Invasive Phragmites Australis in Coastal Wetlands," *International Journal of Remote Sensing*, Vol. 38, No. 8–10, October 2016, pp. 2199–2217.

[4]Colomina, I. and Molina, P., "Unmanned Aerial Systems for Photogrammetry and Remote Sensing: A Review," *Journal of Photogrammetry and Remote Sensing*, Vol. 92, June 2014, pp. 79–97.

[5]Gomez, C. and Purdie, H., "UAV-based Photogrammetry and Geocomputing for Hazards and Disaster Risk Monitoring – A Review," *Geoenvironmental Disasters*, Vol. 3, No. 1, November 2016, pp. 1–11.

[6]Yeong, S. P., King, L. M., and Dol, S. S., "A Review on Marine Search and Rescue Operations Using Unmanned Aerial Vehicles," *International Journal of Mechanical, Aerospace, Industrial, Mechatronic and Manufacturing Engineering*, Vol. 9, No. 2, November 2015, pp. 396–399.

[7]Waharte, S. and Trigoni, N., "Supporting Search and Rescue Operations with UAVs," *International Conference on Emerging Security Technologies*, Canterbury, United Kingdom, September 2010, pp. 142–147.

[8]Nex, F. and Remondino, F., "UAV for 3D Mapping Applications: a Review," *Applied Geomatics*, Vol. 6, No. 1, November 2013, pp. 1–15.

[9]Gatziolis, D., Lienard, J. F., Vogs, A., and Strigul, N. S., "3D Tree Dimensionality Assessment Using Photogrammetry and Small Unmanned Aerial Vehicles," *PLOS ONE*, Vol. 10, No. 9, September 2015, pp. 1–21.

[10]"Concept of operations for the Next Generation Air Transportation System," Version 3.2, Joint Planning and Development Office, Washington, DC, September 2010, `http://www.dtic.mil/dtic/tr/fulltext/u2/a535795.pdf`.

[11]Xargay, E., Kaminer, I., Pascoal, A. M., Hovakimyan, N., Dobrokhodov, V., Cichella, V., Aguiar, A. P., and Ghabcheloo, R., "Time-Critical Cooperative Path Following of Multiple Unmanned Aerial Vehicless over Time-Varying Networks," *Journal of Guidance, Control and Dynamics*, Vol. 36, No. 2, March–April 2013, pp. 499–516.

[12]Xargay, E., *Time-Critical Cooperative Path-Following Control of Multiple Unmanned Aerial Vehicles*, Ph.D. thesis, University of Illinois at Urbana-Champaign, Urbana, Illinois, 2013.

[13]Xargay, E., Choe, R., Hovakimyan, N., and Kaminer, I., "Multi-leader coordination algorithm for networks with switching topology and quantized information," *Automatica*, Vol. 50, No. 3, March 2014, pp. 841–851.

[14]Puig-Navarro, J., Xargay, E., Choe, R., and Hovakimyan, N., "Time-Critical Coordination of Multiple UAVs with Absolute Temporal Constraints," *AIAA Guidance, Navigation and Control Conference*, Kissimmee, FL, January 2015, AIAA 2015-0595.

[15]McLain, T. W. and Beard, R. W., "Coordination Variables, Coordination Functions, and Cooperative Timing Missions," *Journal of Guidance, Control and Dynamics*, Vol. 28, No. 1, January–February 2005, pp. 150–161.

[16]Ghabcheloo, R., Pascoal, A. M., Silvestre, C., and Kaminer, I., "Coordinated Path Following Control of Multiple Wheeled Robots Using Linearization Techniques," *International Journal of Systems Science*, Vol. 37, No. 6, May 2005, pp. 399–414.

[17]Skjetne, R., Moi, S., and Fossen, T. I., "Nonlinear Formation Control of Marine Craft," *IEEE Conference on Decision and Control*, Vol. 2, Las Vegas, NV, December 2002, pp. 1699–1704.

[18]Ihle, I.-A. F., *Coordinated Control of Marine Craft*, Ph.D. thesis, Norwegian University of Science and Technology, Trondheim, Norway, September 2006.

[19]Peyami, E. and Fossen, T. I., "Motion Control of Marine Craft Using Virtual Positional and Velocity Constraints," *International Conference on Control and Automation*, Santiago, Chile, December 2011, pp. 410–416.

[20]Kaminer, I., Yakimenko, O. A., Pascoal, A. M., and Ghabcheloo, R., "Path Generation, Path Following and Coordinated Control for Time-Critical Missions of Multiple UAVs," *American Control Conference*, Mineapolis, MN, June 2006, pp. 4906–4913.

[21]Xargay, E., Choe, R., Hovakimyan, N., and Kaminer, I., "Convergence of a PI Coordination Protocol in Networks with Switching Topology and Quantized Measurements," *IEEE Conference on Decision and Control*, Maui, HI, December 2012, pp. 6107–6112.

[22]Cichella, V., Kaminer, I., Dobrokhodov, V., Xargay, E., Choe, R., Hovakimyan, N., Aguiar, A. P., and Pascoal, A., "Cooperative Path-Following Control of Multiple Multirotors Over Faulty Networks," *IEEE Transactions on Automation Science and Engineering*, Vol. 12, No. 3, July 2015, pp. 945–957.

[23]Choe, R., Puig-Navarro, J., Cichella, V., Xargay, E., and Hovakimyan, N., "Cooperative Trajectory Generation Using Pythagorean Hodograph Bézier Curves," *Journal of Guidance, Control and Dynamics*, Vol. 39, No. 8, August 2016, pp. 1744–1763.

[24]Choe, R., *Distributed Cooperative Trajectory Generation for Multiple Autonomous Vehicles Using Pythagorean Hodograph Bézier Curves*, Ph.D. thesis, University of Illinois at Urbana-Champaign, Urbana, Illinois, 2017.

[25]Bachman, G., Narici, L., and Beckenstein, E., *Fourier and Wavelet Analysis*, Springer, New York, USA, 2000.

[26]Arcak, M., "Passivity as a Design Tool for Group Coordination," *IEEE Transactions on Automatic Control*, Vol. 52, No. 8, August 2007, pp. 1380–1390.

[27]Studinger, M., "Operation IceBridge – Personal Blog," `http://blogs.nasa.gov/icebridge/tag/studinger/`, [Online; accessed 28 April 2016].

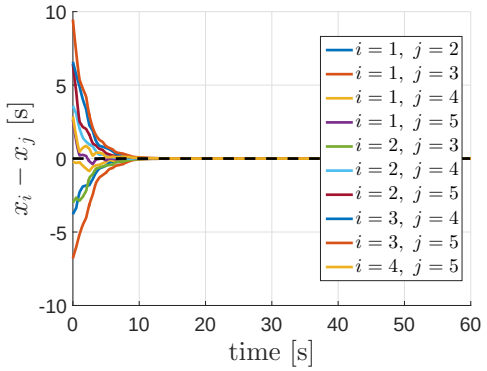

(a) ICE, tight coordination.

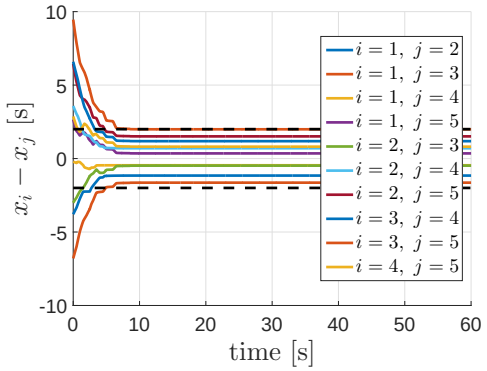

(b) ICE, loose coordination.

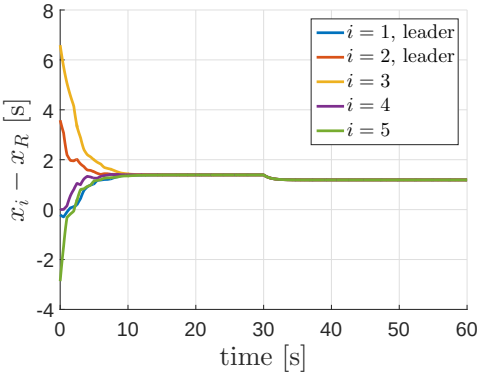

(c) VTE, tight coordination.

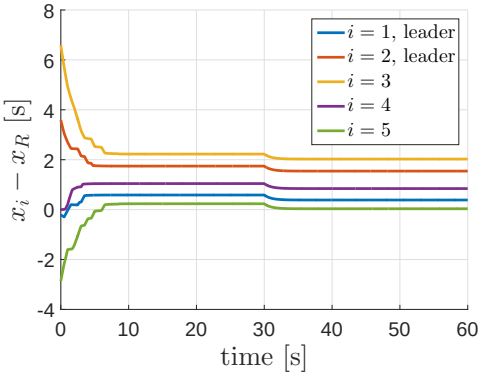

(d) VTE, loose coordination.

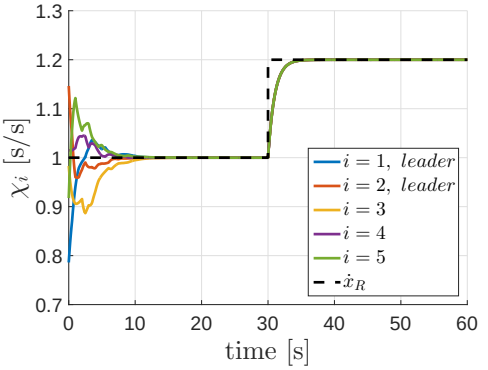

(e) Integral states, tight coordination.

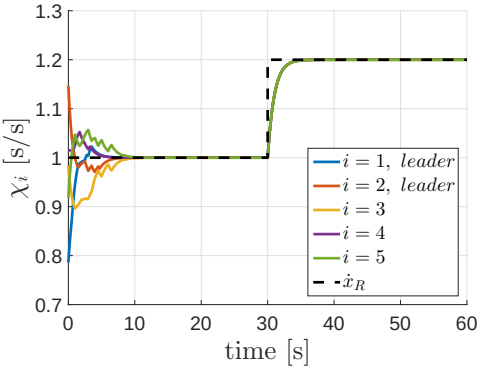

(f) Integral states, loose coordination.

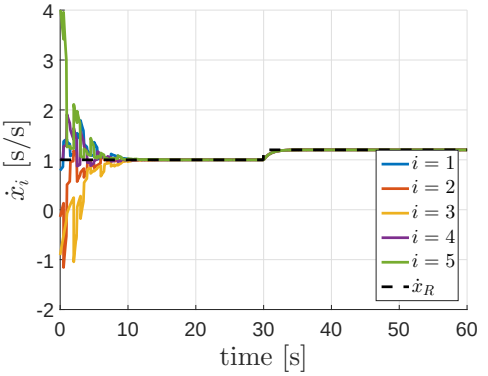

(g) Coordination-state rates, tight coordination.

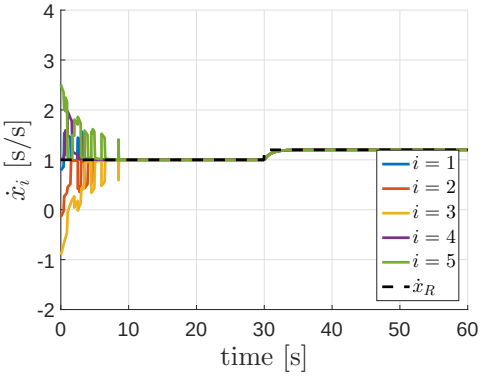

(h) Coordination-state rates, loose coordination.

Figure 9: Unenforced temporal constraints.

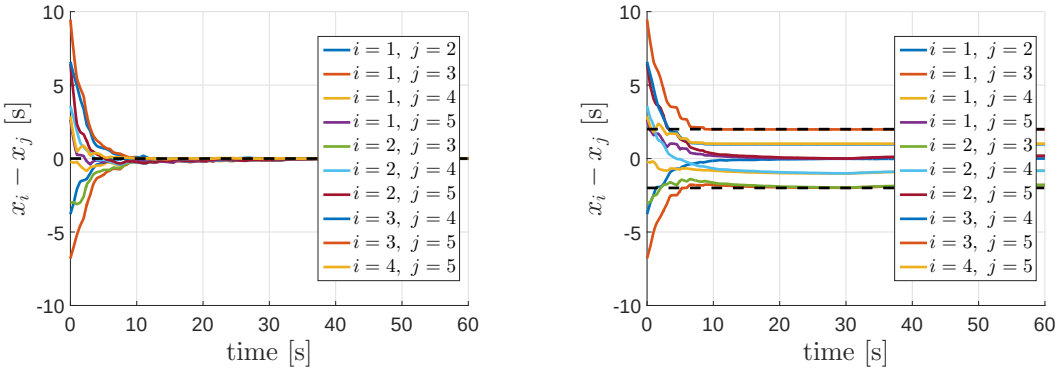

(a) ICE, tight coordination.

(b) ICE, loose coordination.

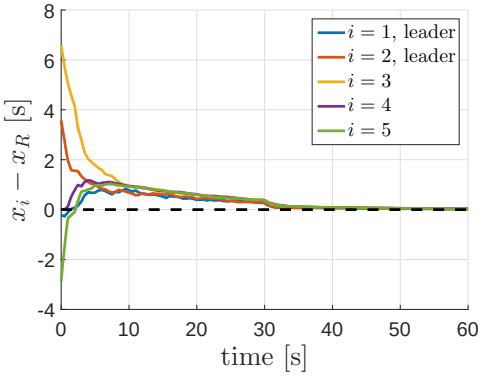

(c) VTE, tight coordination.

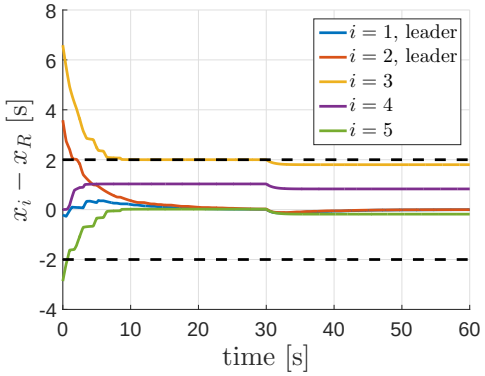

(d) VTE, loose coordination.

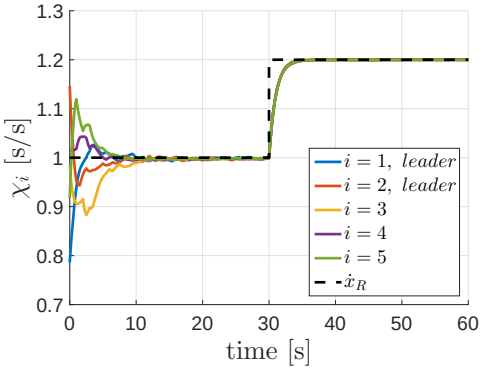

(e) Integral states, tight coordination.

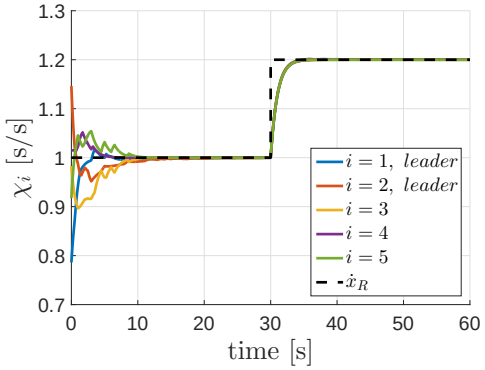

(f) Integral states, loose coordination.

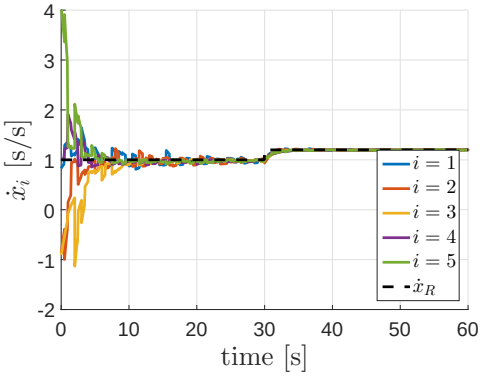

(g) Coordination-state rates, tight coordination.

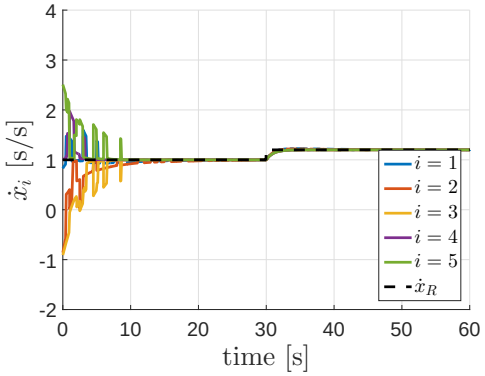

(h) Coordination-state rates, loose coordination.

Figure 10: Strict temporal constraints.

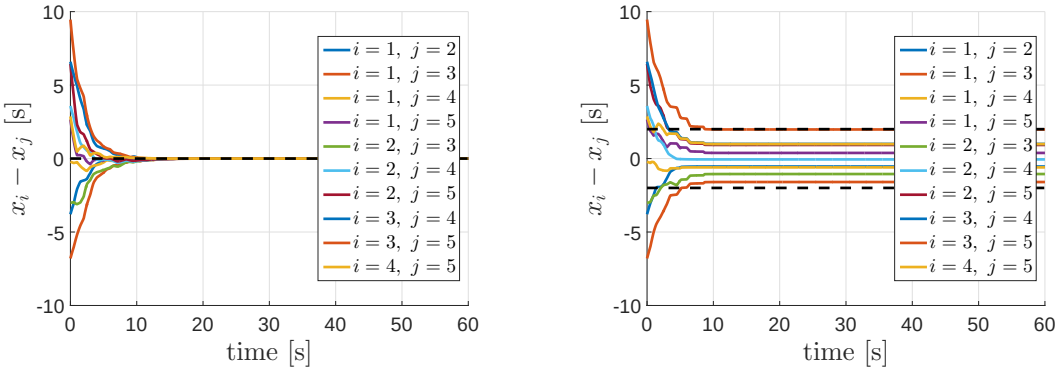

(a) ICE, tight coordination.

(b) ICE, loose coordination.

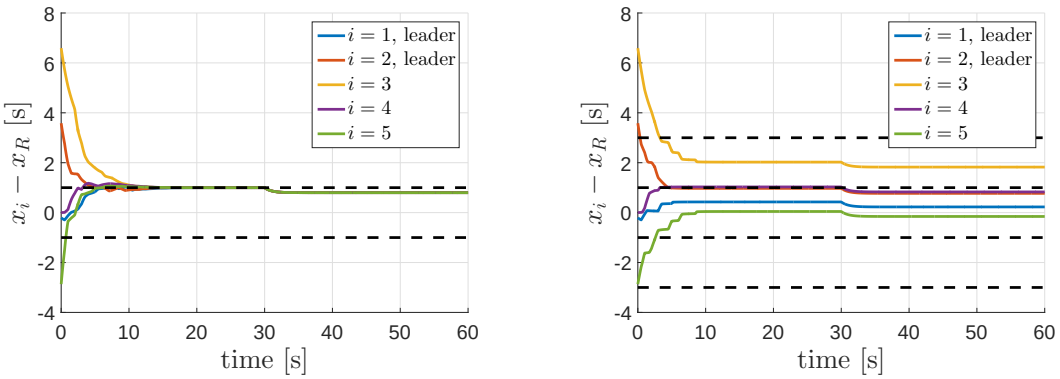

(c) VTE, tight coordination.

(d) VTE, loose coordination.

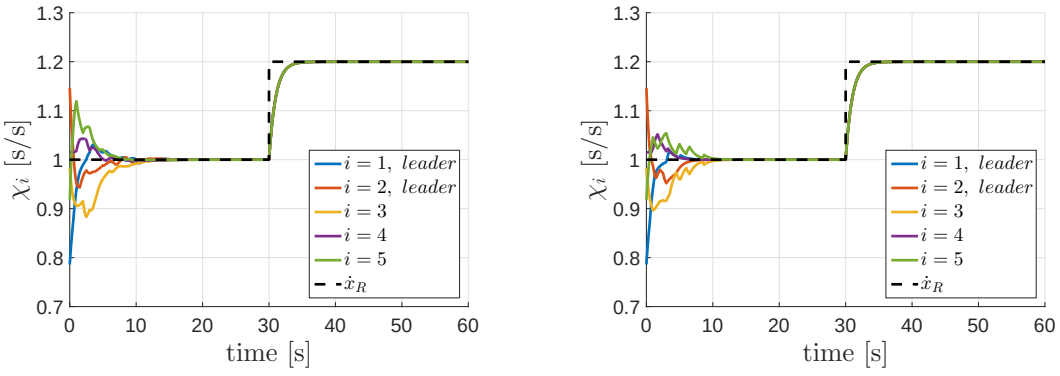

(e) Integral states, tight coordination.

(f) Integral states, loose coordination.

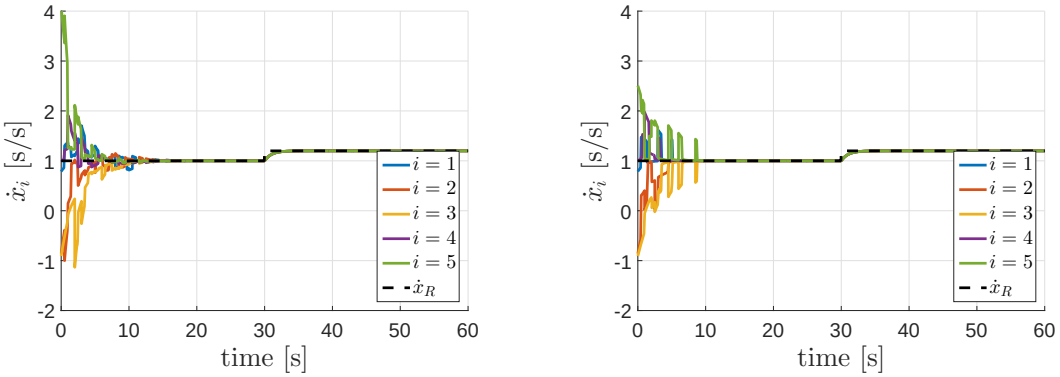

(g) Coordination-state rates, tight coordination.

(h) Coordination-state rates, loose coordination.

Figure 11: Relaxed temporal constraints.